Damping Torque Analysis of Power Systems with DFIGs for Wind Power Generation

Du, W., Bi, J., Lv, C., & Littler, T. (2016). Damping Torque Analysis of Power Systems with DFIGs for Wind Power Generation. IET Renewable Power Generation. DOI: 10.1049/iet-rpg.2016.0139

Published in:
IET Renewable Power Generation

Document Version:
Peer reviewed version

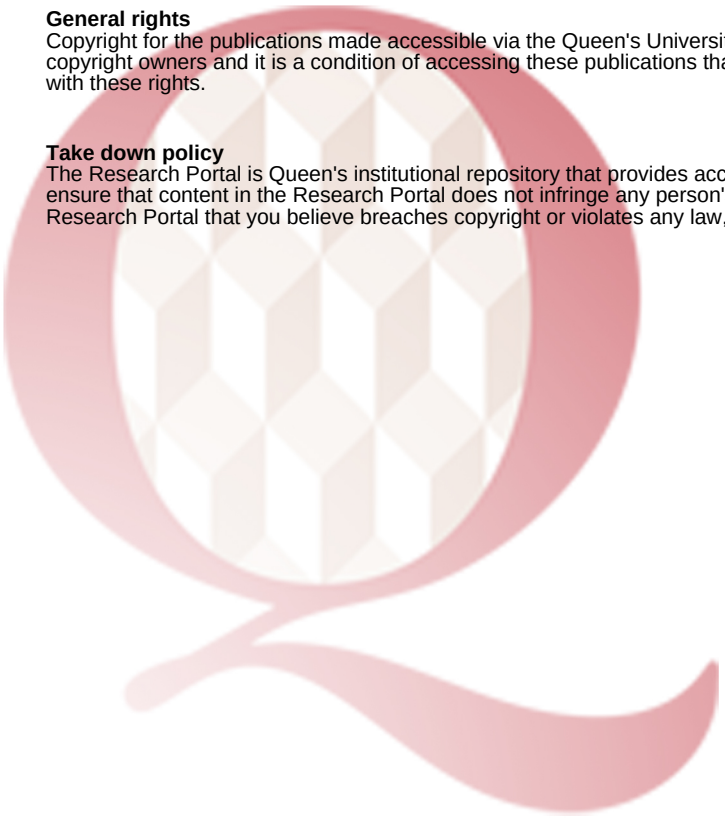

Damping Torque Analysis of Power Systems with DFIGs for Wind Power Generation

Wenjuan Du [1], Jingtian Bi [1], Chen Lv [2*], and Tim Littler [2]

[1] The state the State Key Laboratory of Alternate Electric Power Systems with New Energy Resources, North China Electric Power University, Changping, Beijing, China.
[2] School of Electronic, Electrical Engineering and Computer Science, the Queen's University of Belfast, Belfast, UK
[*] clv01@qub.ac.uk

Abstract: A grid-connected DFIG for wind power generation can affect power system small-signal angular stability in two ways: by changing the system load flow condition and dynamically interacting with synchronous generators (SGs). This paper presents the application of conventional method of damping torque analysis (DTA) to examine the effect of DFIG's dynamic interactions with SGs on the small-signal angular stability. It shows that the effect is due to the dynamic variation of power exchange between the DFIG and power system and can be estimated approximately by the DTA. Consequently, if the DFIG is modelled as a constant power source when the effect of zero dynamic interactions is assumed, the impact of change of load flow brought about by the DFIG can be determined. Thus the total effect of DFIG can be estimated from the result of DTA added on that of constant power source model. Applications of the DTA method proposed in the paper are discussed. An example of multi-machine power systems with grid-connected DFIGs are presented to demonstrate and validate the DTA method proposed and conclusions obtained in the paper.

Key words: Power system small-signal angular stability, the DFIG, Heffron-Phillips model, damping torque analysis (DTA).

Nomenclature

p	Laplace operator or d/dt.
Δ	Small increment or dynamic variation of a variable.
0	Subscript denotes the value of a variable at steady state
$-$	Upper bar indicates a phasor or complex number.
d,q	Subscript indicates d or q component of a phasor under machine's reference coordinate.
x,y	Subscript indicates x or y component of a phasor under system common reference coordinate.
s	Slip of DFIG generator.
$\bar{E}'_w$	Rotor transient EMF of a DFIG generator.
$\bar{V}_r$	Rotor voltage of a DFIG generator.

1. Introduction

Variable speed wind generators, such as DFIGs, are connected to a power system through power electronics based converters. Their dynamic interactions with the power system are different to that of conventional synchronous generators (SGs). Grid connection of wind generators may either displace conventional synchronous machines to retire or simply to meet system load increase without displacing

any SGs. In both cases, large-scale grid integration of variable speed wind generators may pose a threat to the security of power system operation. One particular concern is the damping of power system low-frequency oscillations as affected by grid-connected wind generators. This important issue can be studied by examining the system small-signal angular stability, which has been a subject of investigation in many recent publications [1]-[8].

Authors of [1] have thoughtfully summarized three main factors that a grid-connected DFIG may affect the damping of power system oscillations: (1) displacing a synchronous generator; (2) changing system load flow; (3) dynamically interacting with synchronous generators. Each of those factors can influence power system small-signal angular stability differently. Earlier work presented in [2] and [3] has adopted an approach of displacing synchronous machines by the DFIGs to investigate the impact of wind penetration on power system small-signal angular stability. [4] and [5] further extend the strategy of displacement to investigate the effect of supplementary reactive power/voltage control of DFIGs on power system small-signal angular stability. Useful conclusions are presented in [4] and [5] for guiding how increased wind penetration can safely replace conventional generation in the power system. The case of increased wind penetration to meet the load requirement without displacing any SGs has been investigated in [6]-[8]. Grid integration of a DFIG changes system load flow and introduces dynamic interactions with SGs at the same time. It will be useful if a method can be developed to individually examine the impact of each of those two affecting factors of the DFIG on power system small-signal angular stability.

This paper considers grid connection of DFIGs to meet the load increase without displacing any conventional SGs. Main contribution of the paper is the application of conventional method of damping torque analysis (DTA) to estimate the impact of DFIG's dynamic interactions with the SGs on power system electromechanical oscillation modes. In order to clearly demonstrate the procedure of applying the DTA method, Heffron-Phillips model of a multi-machine power system [9]-[13] with a grid-connected DFIG is established. In the established model, DFIG is treated as a feedback controller expressed by its transfer functions. Thus the impact of DFIG's dynamic interactions with the SGs can be estimated to be its damping torque contributions to affect the system oscillation modes. It is demonstrated in the paper that when the dynamic interactions are assumed to be zero, the DFIG is degraded into a constant power source to affect power system load flow only. Thus it is concluded that the DFIG's impact due to the change of load flow can be estimated by modelling it as the constant power source. Separate examination of two affecting factors of DFIG on power system small-signal angular stability is achieved. This provides a way for gaining better understanding and deeper insight into the mechanism on how grid-connected DFIGs affect the power system small-signal angular stability.

2. Damping torque analysis for a grid-connected DFIG

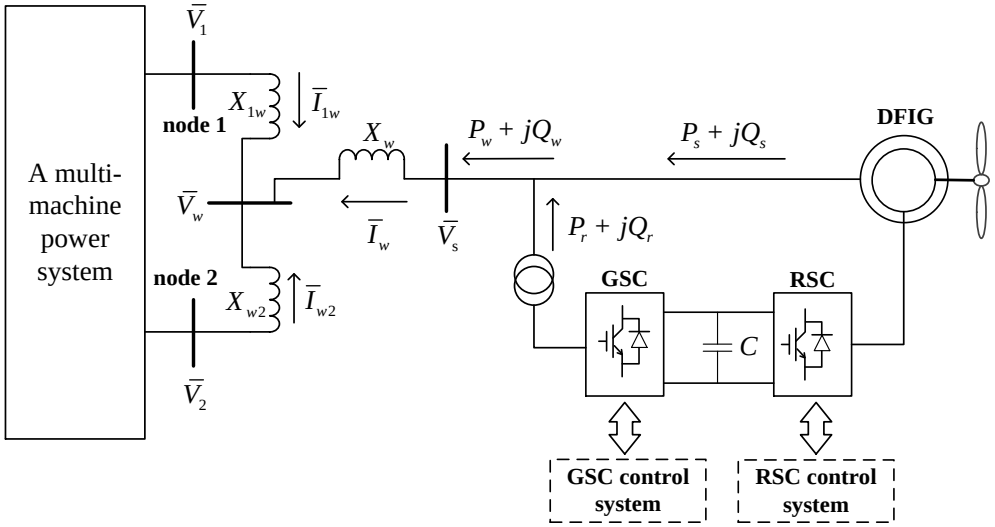

Fig. 1. *A DFIG connected to a multi-machine power system*

Figure 1 shows the configuration of a DFIG connected to a multi-machine power system. In Fig. 1, $P_w + jQ_w$ is the injection of complex power from the DFIG into power system which is the physical cause of existence of interactions between the DFIG and power system for the DFIG to affect system small-signal angular stability. $P_w + jQ_w$ can be written as

$$P_w + jQ_w = P_{w0} + jQ_{w0} + \Delta P_w + j\Delta Q_w \tag{1}$$

where $\Delta P_w + j\Delta Q_w$ is the dynamic variation of the complex power when the system is subject to small disturbances. $\Delta P_w + j\Delta Q_w$ exists as the result of dynamic interactions between the DFIG and power system. It is the key element to determine how the DFIG's dynamic interactions with power system affect system small-signal angular stability. In this section, the DTA is applied to estimate how much the effect of $\Delta P_w + j\Delta Q_w$ is on power system electromechanical oscillation modes. In the assumed case that DFIG's dynamic interactions do not exist, $\Delta P_w + j\Delta Q_w = 0$. Eq.(1) indicates that in this case the DFIG becomes a constant power source $P_{w0} + jQ_{w0}$. This is when the DFIG affects system small-signal angular stability by changing the system load flow only. Hence the impact of load flow change introduced by the DFIG on oscillation modes can be individually estimated by modelling the DFIG as the constant power source.

In order to demonstrate in details how the strategy outlined above can be implemented to separately examine the impact of dynamic interactions and load flow change brought about by the DFIG, in this section, firstly the Heffron-Phillips dynamic model of the power system of Fig. 1 is established. Secondly the DTA is applied to give the estimation of the impact of DFIG's dynamic interactions with power

system. Finally, potential applications of examining the impact of load flow change introduced by the DFIG are discussed.

2.1. Heffron-Phillips model

The linearized model of a multi-machine power system with a grid-connected DFIG can be established to be

$$\frac{d}{dt}\begin{bmatrix} \Delta\boldsymbol{\delta} \\ \Delta\boldsymbol{\omega} \\ \Delta\boldsymbol{E}_q' \\ \Delta\boldsymbol{E}_{fd}' \end{bmatrix} = \begin{bmatrix} \boldsymbol{0} & \boldsymbol{\omega_o I} & \boldsymbol{0} & \boldsymbol{0} \\ \boldsymbol{-M^{-1}K_1} & \boldsymbol{-M^{-1}D} & \boldsymbol{-M^{-1}K_2} & \boldsymbol{0} \\ \boldsymbol{-T_{d0}^{-1}K_4} & \boldsymbol{0} & \boldsymbol{-T_{d0}^{-1}K_3} & \boldsymbol{T_{d0}^{-1}} \\ \boldsymbol{-T_A^{-1}K_5K_A} & \boldsymbol{0} & \boldsymbol{-T_A^{-1}K_6K_A} & \boldsymbol{-T_A^{-1}} \end{bmatrix} \begin{bmatrix} \Delta\boldsymbol{\delta} \\ \Delta\boldsymbol{\omega} \\ \Delta\boldsymbol{E}_q' \\ \Delta\boldsymbol{E}_{fd}' \end{bmatrix} + \begin{bmatrix} \boldsymbol{0} \\ \boldsymbol{-M^{-1}k_{PP}} \\ \boldsymbol{-T_{d0}^{-1}k_{EP}} \\ \boldsymbol{T_A^{-1}K_Ak_{VP}} \end{bmatrix} \Delta P_w + \begin{bmatrix} \boldsymbol{0} \\ \boldsymbol{-M^{-1}k_{PQ}} \\ \boldsymbol{-T_{d0}^{-1}k_{EQ}} \\ \boldsymbol{T_A^{-1}K_Ak_{VQ}} \end{bmatrix} \Delta Q_w \tag{2}$$

which can be written as

$$\frac{d}{dt}\Delta\boldsymbol{X_g} = \boldsymbol{A_g}\Delta\boldsymbol{X_g} + \boldsymbol{b_P}\Delta P_w + \boldsymbol{b_Q}\Delta Q_w \tag{3}$$

where state variables and elements of state matrix are as same as those defined in the conventional Heffron-Phillips model of a multi-machine power system [9]-[14].

Denote V_s the magnitude of voltage at the node in the power system to which the DFIG is connected (PCC). It can have

$$\Delta V_s = \boldsymbol{C_g}\Delta\boldsymbol{X_g} + d_{g1}\Delta P_w + d_{g2}\Delta Q_w \tag{4}$$

In Eq.(4), $\boldsymbol{C_g} = \begin{bmatrix} \boldsymbol{c_{g1}} & \boldsymbol{0} & \boldsymbol{c_{g3}} & \boldsymbol{0} \end{bmatrix}$, where $\boldsymbol{c_{g1}}$ and $\boldsymbol{c_{g3}}$ is the coefficient vector corresponding to $\Delta\boldsymbol{\delta}$ and $\Delta\boldsymbol{E_q'}$, respectively.

Linearized model of the DFIG is

$$\begin{aligned} \frac{d}{dt}\Delta E_{wd}' &= K_{w1}\Delta E_{wd}' + K_{w2}\Delta E_{wq}' + K_{w3}\Delta s + K_q\Delta V_{rq} \\ \frac{d}{dt}\Delta E_{wq}' &= K_{w4}\Delta E_{wd}' + K_{w5}\Delta E_{wq}' + K_{w6}\Delta s + K_{qV}\Delta V_s + K_d\Delta V_{rd} \\ \frac{d}{dt}\Delta s &= K_{w7}\Delta E_{wd}' + K_{w8}\Delta E_{wq}' + K_{sV}\Delta V_s \end{aligned} \tag{5}$$

where

$$\begin{aligned} \Delta V_{rd} &= K_{d1}(p)\Delta E_{wd}' + K_{d2}(p)E_{wq}' + K_{d3}\Delta s + K_{d4}(p)\Delta V_s \\ \Delta V_{rq} &= K_{q1}(p)\Delta E_{wd}' + K_{q2}(p)\Delta E_{wq}' + K_{q3}\Delta s + K_{q4}(p)\Delta V_s \end{aligned} \tag{6}$$

In matrix form, Eq.(5) and (6) can be written together as

$$\frac{d}{dt}\Delta\boldsymbol{X_w} = \boldsymbol{A_w}(p)\Delta\boldsymbol{X_w} + \boldsymbol{b_w}(p)\Delta V_s \tag{7}$$

Linearization of power output from the DFIG can be obtained to be

$$\begin{bmatrix}\Delta P_w\\ \Delta Q_w\end{bmatrix}=\begin{bmatrix}\boldsymbol{c}_{Pw}{}^{T}\\ \boldsymbol{c}_{Qw}{}^{T}\end{bmatrix}\boldsymbol{\Delta X}_w+\begin{bmatrix}c_{PV}\\ c_{QV}\end{bmatrix}\Delta V_s \tag{8}$$

Detailed derivation of Eq.(2) and (4) is given in Appendix A. That of Eq.(5) , (6) and (8) is given in Appendix B.

From Eq.(7) and (8) it can have

$$\begin{aligned}\Delta P_w &= \{\boldsymbol{c}_{Pw}{}^{T}[p\boldsymbol{I}-\boldsymbol{A}_W(p)]^{-1}\boldsymbol{b}_w(p)+c_{PV}\}\Delta V_s = G_{wP}(p)\Delta V_s\\ \Delta Q_w &= \{\boldsymbol{c}_{Qw}{}^{T}[p\boldsymbol{I}-\boldsymbol{A}_W(p)]^{-1}\boldsymbol{b}_w(p)+c_{QV}\}\Delta V_s = G_{wQ}(p)\Delta V_s\end{aligned} \tag{9}$$

Equation (3), (4) and (9) together form the Heffron-Phillips model of the multi-machine power system with the grid-connected DFIG, which can be shown by Fig. 2 and 3. In the model, Eq.(3) is the "open-loop" state equation and (4) the output equation. The DFIG is treated as a one-input two-output "feedback controller" shown by Eq.(9), Fig. 2 and 3. Hence Eq. (3) and (4) form the "closed-loop" system model together with Eq.(9).

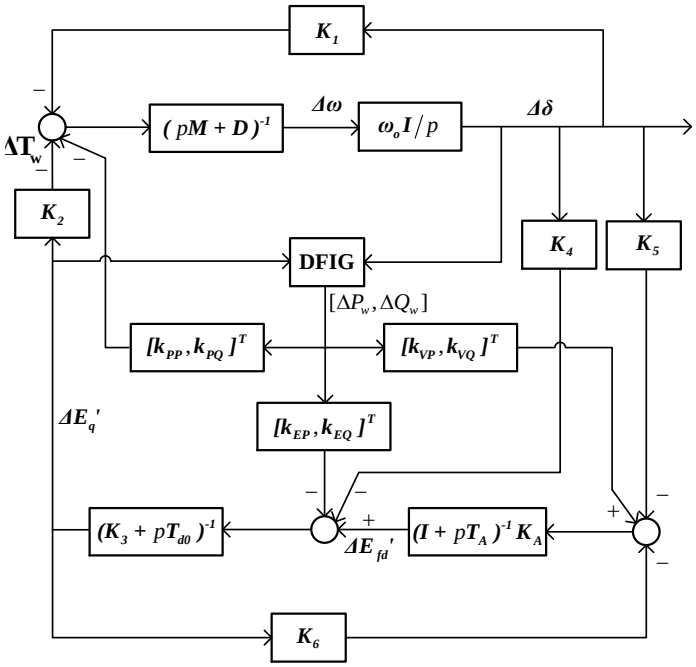

Fig. 2. *Heffron-Phillips model of a multi-machine power system with the grid-connected DFIG–part of the power system*

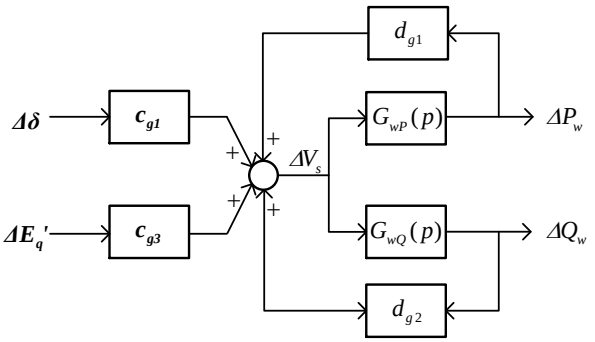

Fig. 3. *Heffron-Phillips model of a multi-machine power system with the grid-connected DFIG–part of the DFIG*

Heffron-Phillips model has been used for examining the damping torque contribution from a power system controller, such as a power system stabilizer (PSS), to affect power system electromechanical oscillation modes [9]-[13]. The model shown by Fig. 2 and 3 for the grid-connected DFIG is derived, aiming at the estimation of impact of DFIG's dynamic interactions with the power system. Hence ΔP_w and ΔQ_w are selected as the output signals from the DFIG. The novelty of derived model, firstly, is the demonstration that the DFIG can be treated as feedback controller such that its impact can be estimated by use of the damping torque analysis, which will be presented in the next subsection. Secondly, the derivation of the model indicates that ΔP_w and ΔQ_w only respond to the variation of magnitude of DFIG's terminal voltage, ΔV_s, as shown by Eq.(9) and Fig. 3. This result is meaningful because in the small-signal analysis using linearized model, error of phase tracking of voltage $\bar{V}_s$ by the phase-locked loop (PLL) is not considered at all. The only error signal "seen" by the DFIG is the deviation of voltage magnitude at the PCC. Normally ΔV_s is small, ΔP_w and ΔQ_w are limited. Hence it is expected that the impact of DFIG's dynamic interactions with power system on system small-signal angular stability normally should be small. This is quite similar to the voltage control function of a static Var compensator (SVC) or static synchronous compensator (STATCOM). Previous study has confirmed that the voltage control function of the SVC and STATCOM has little effect on the damping of power system oscillations [15]-[18].

2.2. Damping torque analysis

Transfer function matrix from the DFIG outputs, ΔP_w and ΔQ_w, to its electric torque contribution to the electromechanical oscillation loop of synchronous generators can be obtained from Fig. 2 to be

$$\begin{aligned}\frac{\Delta \boldsymbol{T}_P}{\Delta P_w} &= \boldsymbol{G}_P(p) = \boldsymbol{k}_{PP} + \boldsymbol{K}(p)^{-1}[(\boldsymbol{I} + p\boldsymbol{T}_A)\boldsymbol{k}_{EP} + \boldsymbol{K}_A\boldsymbol{k}_{VP}] \\ \frac{\Delta \boldsymbol{T}_Q}{\Delta Q_w} &= \boldsymbol{G}_Q(p) = \boldsymbol{k}_{PQ} + \boldsymbol{K}(p)^{-1}[(\boldsymbol{I} + p\boldsymbol{T}_A)\boldsymbol{k}_{EQ} + \boldsymbol{K}_A\boldsymbol{k}_{VQ}]\end{aligned} \tag{10}$$

where $\boldsymbol{K}(p) = \boldsymbol{K}_2[(\boldsymbol{I} + p\boldsymbol{T}_A)(\boldsymbol{K}_3 + p\boldsymbol{T}_{d0}) + \boldsymbol{K}_A\boldsymbol{K}_6]$. Hence the electric torque contribution from the DFIG is

$$\Delta \boldsymbol{T}_w = \Delta \boldsymbol{T}_P + \Delta \boldsymbol{T}_Q = [\boldsymbol{G}_P(p)G_{wP}(p) + \boldsymbol{G}_Q(p)G_{wQ}(p)]\Delta V_s \tag{11}$$

The electric torque provided by the DFIG to the *k*th synchronous generator is

$$\Delta T_{wk} = [g_{Pk}(p)G_{wP}(p) + g_{Qk}(p)G_{wQ}(p)]\Delta V_s \tag{12}$$

where $g_{Pk}(p)$ and $g_{Qk}(p)$ is the *k*th element of $\boldsymbol{G}_P(p)$ and $\boldsymbol{G}_Q(p)$ respectively.

Denote $\bar{\lambda}_i = -\xi_i + j\omega_i$ the *i*th electromechanical oscillation mode of the power system of Fig. 1. It is one of the eigenvalues of state matrix of the closed-loop system model including the DFIG's dynamics of Eq.(9) (not that of open-loop state matrix $\boldsymbol{A}_g$). If $\bar{\boldsymbol{v}}_i$ is the right eigenvector associated with $\bar{\lambda}_i = -\xi_i + j\omega_i$, it can be proved that at $p = \bar{\lambda}_i$ (see Appendix C)

$$\Delta V_s = \frac{1}{1 - d_{g1}\bar{G}_{wP}(\bar{\lambda}_i) - d_{g2}\bar{G}_{wQ}(\bar{\lambda}_i)} \frac{\boldsymbol{C}_g \bar{\boldsymbol{v}}_{ig}}{\bar{v}_{ik}} \Delta\omega_k = \bar{\gamma}_{ik}(\bar{\lambda}_i)\Delta\omega_k \tag{13}$$

where $\bar{\boldsymbol{v}}_{ig}$ is the vector consisted of elements of $\bar{\boldsymbol{v}}_i$ corresponding to $\Delta\boldsymbol{X}_g$, $\bar{v}_{ik}$ is the element of $\bar{\boldsymbol{v}}_i$ corresponding to state variable $\Delta\omega_k$, the deviation of rotor speed of the *k*th synchronous generator in the system. Hence at the complex oscillation frequency $\bar{\lambda}_i = -\xi_i + j\omega_i$, the damping torque provided by the DFIG to the *k*th generator can be obtained from Eq.(12) and (13) to be

$$\Delta T_{wDk} = \mathrm{Re}\{[\bar{g}_{Pk}(\bar{\lambda}_i)\bar{G}_{wP}(\bar{\lambda}_i) + \bar{g}_{Qk}(\bar{\lambda}_i)\bar{G}_{wQ}(\bar{\lambda}_i)]\bar{\gamma}_{ik}(\bar{\lambda}_i)\}\Delta\omega_k = D_{wk}\Delta\omega_k \tag{14}$$

where $\mathrm{Re}\{\}$ denotes the real part of a complex number. Let the sensitivity of the electromechanical oscillation mode to the damping torque coefficient of the *k*th generator be

$$\bar{S}_{ik} = \frac{\partial\bar{\lambda}_i}{\partial D_{wk}} \tag{15}$$

Equation (14) and (15) together gives the estimation of impact of the damping torque contribution from the DFIG on the oscillation mode to be

$$\Delta\bar{\lambda}_i = \sum_{k=1}^{N} \bar{S}_{ik} D_{wk} \tag{16}$$

2.3. Separate examination of the impact of grid-connected DFIG on power system small-signal angular stability

Equation (16) can estimate the impact of DFIG's dynamic interactions with power system on the electromechanical oscillation mode. The impact is due to the dynamic variation of power injection from the DFIG into the power system, ΔP_w and ΔQ_w, or equivalently the inclusion of DFIG's dynamics expressed by its transfer function of Eq.(9). In an assumed case that $\Delta P_w = \Delta Q_w = 0$, the DFIG provides no damping torque to SGs and there exist no dynamic interactions between the DFIG and power system ($\Delta\bar{\lambda}_i = 0$). As pointed out previously, in this case the DFIG is degraded into a constant power injection into the power system, $P_{w0} + jQ_{w0}$. From Eq.(3) it can be seen that the system model becomes

$$\frac{d}{dt}\Delta\boldsymbol{X}_g = \boldsymbol{A}_g\Delta\boldsymbol{X}_g \tag{17}$$

Hence the eigenvalues of open-loop state matrix $\boldsymbol{A}_g$ (denoted as $\bar{\lambda}_{i0}$) are the indications of system small-signal angular stability when the DFIG is modelled as a constant power injection. This means how much the load flow change brought about by the DFIG affects the system small-signal angular stability can be determined by computing $\bar{\lambda}_{i0}$.

With the DFIG's dynamics being considered, $\Delta P_w \neq 0$ or/and $\Delta Q_w \neq 0$. Eigenvalues of state matrix of the closed-loop system model is $\bar{\lambda}_i$. Difference between $\bar{\lambda}_{i0}$ and $\bar{\lambda}_i$ is $\Delta\bar{\lambda}_i$ which is caused by dynamic interactions between the DFIG and power system and can be estimated by the DTA of Eq.(16). Therefore, the power system small-signal angular stability as affected by the DFIG can be examined separately in two steps. Firstly, the DFIG is modelled as a constant power injection and $\bar{\lambda}_{i0}$ is calculated from open-loop state matrix $\boldsymbol{A}_g$ to check how much the load flow change introduced by the DFIG influences system stability. Secondly, $\Delta\bar{\lambda}_i$ is calculated by using the DTA of Eq.(16) to see how much the effect of the dynamic interactions between the DFIG and synchronous generators is.

Estimation of dynamic interactions of the DFIGs with the SGs is important to understand the change of behavior of the power system when the DFIGs get involved. In [5] and [8], it was proposed that the participation factors of state variables of the DFIGs are calculated to estimate the scale of involvement of the DFIGs in power system electromechanical oscillation modes. However, the participation factors can only examine the scale of DFIG's involvement in a particular electromechanical oscillation mode of interests. $\Delta\bar{\lambda}_i$ by applying the DTA as proposed in this paper can give the estimation of not only the scale, but also the direction of DFIG's dynamic engagement in the oscillation mode, i.e., positive to enhance or negative to reduce the damping of oscillation mode of interests.

As pointed out and discussed previously in this section, Eq.(9) indicates that dynamic interactions of DFIG's with power system should normally be limited as in power systems, ΔV_s usually is small. Hence the impact of dynamic interactions as measured by $\Delta\bar{\lambda}_i$ is small. This means that if the impact of grid connection of DFIG on power system small-signal angular stability is significant, it normally should be due to the change of load flow brought about by the DFIG. This conclusion is useful in planning the grid connection of wind farms when their dynamic models are normally not available. By modelling wind farms as constant power sources and computing the oscillation modes from system open-loop state matrix $\boldsymbol{A}_g$, the most dangerous scenarios of connections of wind farms can be found.

3. An Example

Configuration of a 16-machine 68-bus test power system is shown by Fig. 4. In this example, the 7th-order model of SG, 2nd-order model of the AVR and 2nd-order model of the PSS were used. The loads were modelled as constant impedance. Parameters of the system and synchronous generators are given in [20]. There are four inter-area oscillation modes in the power system crucial to the small-signal angular stability of example system, which are listed in Table 1.

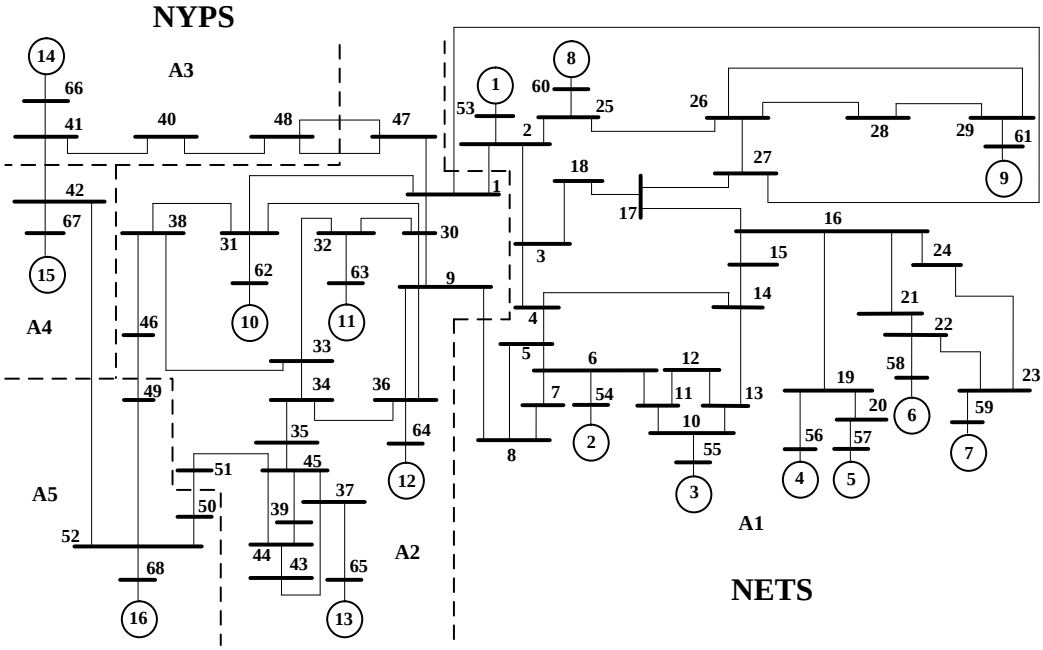

Fig. 4. *Configuration of 16-machine 68-bus test power system*

In order to demonstrate the application of the proposed method, it is assumed that a wind farm represented by a DFIG is to be connected at node 8 of the example power system without displacing any synchronous generators. Parameters of the DFIG are given in Appendix D. Load flow change introduced by the DFIG is balanced by G13.

Table 1 Inter-area Modes of 16-machine 68-bus Test Power System

Mode i	Value
1	-0.1222 + 3.6351i
2	-0.3165 + 3.1942i
3	-0.0941 + 2.7222i
4	-0.1512 + 2.0486i

Firstly, the DFIG was modelled as a constant power injection $P_{w0} + jQ_{w0}$. P_{w0} increases from $P_{w0} = 0$ to $P_{w0} = 3$ consecutively and Q_{w0} changes accordingly with a fixed power factor of 0.95. Changes of four

inter-area oscillation modes, $\bar{\lambda}_{i0}, i=1,2,3,4$, can be calculated from open-loop system state matrix $\boldsymbol{A}_g$ and are displayed in Fig. 5 as solid curves, where the arrows show the direction of change of $\bar{\lambda}_{i0}, i=1,2,3,4$ when P_{w0} increased.

Secondly, the DTA was applied to calculate the effect of dynamic interactions between the DFIGs and synchronous generators. Results of variations of four inter-area oscillation modes as affected by the DFIGs are shown as $\Delta\bar{\lambda}_i, i=1,2,3,4$ in Fig. 5. Results of $\bar{\lambda}_{i0}+\Delta\bar{\lambda}_i, i=1,2,3,4$ are presented in Fig. 5 as dashed curves respectively.

Finally, to confirm those results, closed-loop system model of Eq.(1), (2) and (8) with DFIGs' dynamics included was used to calculate the oscillation modes of the system. The inter-area oscillation modes were calculated to be $\bar{\lambda}_i, i=1,2,3,4$ and displayed as dashed curves with crosses in Fig. 5.

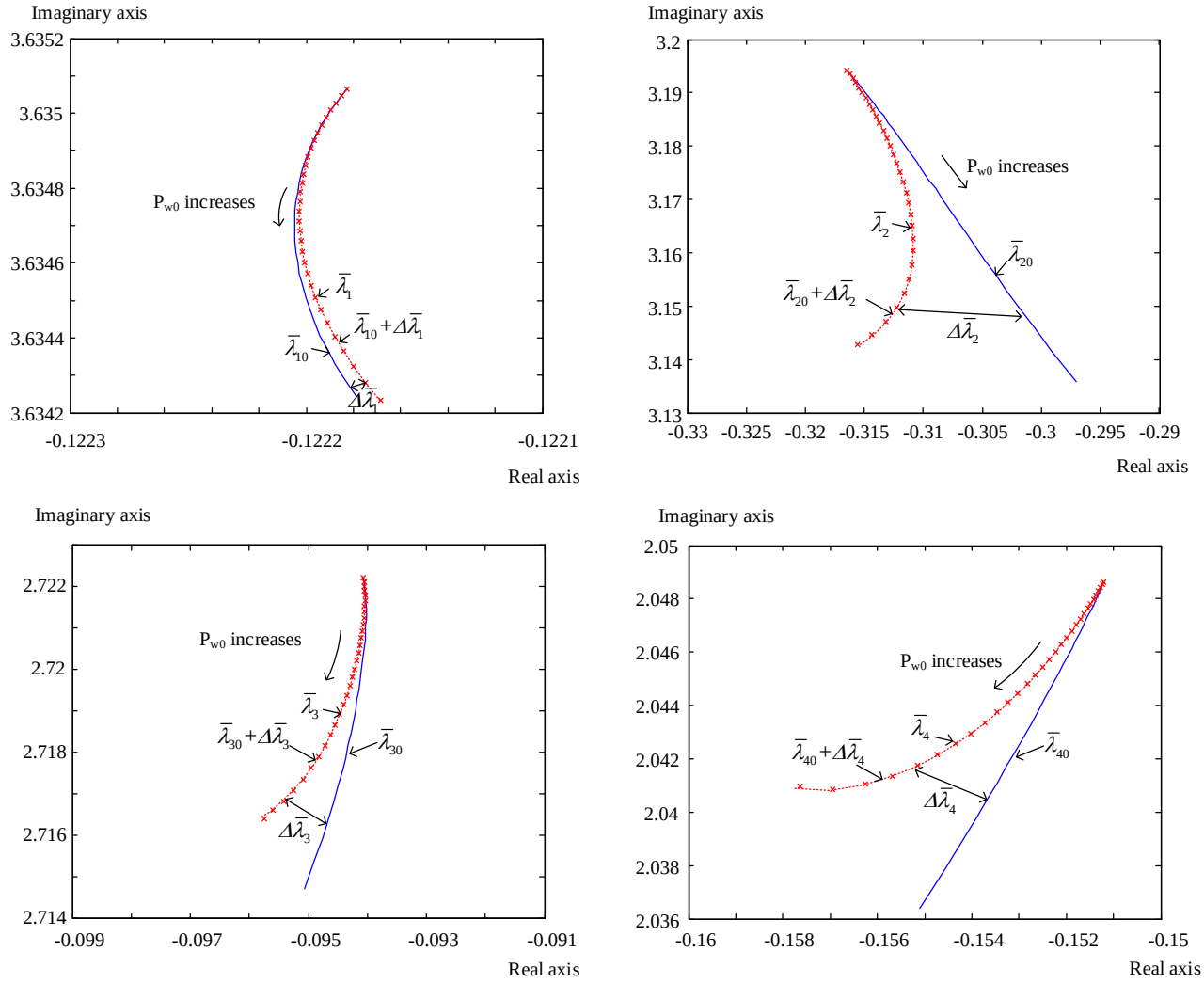

Fig. 5. *Trajectory of inter-area oscillation modes when the level of wind penetration increases with the DFIG being connected at node 8*

From Fig. 5 it can be seen that variation of damping of oscillation modes $\bar{\lambda}_i, i=1,2,3,4$ as affected by the DFIGs is approximately equal to that caused by the dynamic interactions between the DFIGs and synchronous generators $\Delta\bar{\lambda}_i, i=1,2,3,4$ and in addition to that by the load flow change introduced by the DFIGs $\bar{\lambda}_{i0}, i=1,2,3,4$. Hence correctness of the method proposed in the previous section is confirmed.

From Fig. 5 it can also be seen that the effect of dynamic interactions between the DFIG and synchronous generators on the damping of oscillation mode 1 is negative but rather limited; that on the damping of mode 2, 3 and 4 is slightly bigger and positive, but still very small. As normally the effect of dynamic interactions introduced by the DFIGs on power system small-signal angular stability is small, the changes of the oscillation modes are mainly due to the effect of load flow brought about by the DFIGs when they are significant. Hence when the impact of wind power connections is examined, the wind power generation can be modelled as constant power injection firstly. By changing the amount of wind power injection, the most dangerous scenarios of system operation with wind power connections can be identified via calculating $\bar{\lambda}_{i0}$.

To demonstrate this conclusion further, another candidate DFIG connection location, node 16, is also considered. When the output power of DFIG is set to 3 pu, the effect of load flow brought about by the DFIG at node 8 and node 16 $\bar{\lambda}_{i0}$ is listed in Table 2. The accurate results (with DFIG's dynamics being included) of inter-area oscillation modes as effected by DFIG at node 8 and node 16 $\bar{\lambda}_i$ are also listed in Table 3.

Table 2 Effect of Load Flow Brought About by the DFIG Connected at Node 8 and Node 16

	Mode 1	Mode 2	Mode 3	Mode 4
Node 8	-0.1222 + j3.6342	-0.2970 + j3.1359	-0.0951 + j2.7147	-0.1551 + j2.0364
Node 16	-0.1221 + j3.6342	-0.2884 + j3.1158	-0.0959 + j2.7127	-0.1564 + j2.0283

Table 3 Inter-area Oscillation Modes with the DFIG Connected at Node 8 and Node 16

	Mode 1	Mode 2	Mode 3	Mode 4
Node 8	-0.1222 + j3.6342	-0.3156 + j3.1429	-0.0957 + j2.7164	-0.1576 + j2.0410
Node 16	-0.1222 + j3.6342	-0.3113 + j3.1236	-0.0967 + j2.7145	-0.1616 + j2.0328

From Table 3, it can be seen that: (1) Among four inter-area oscillation modes, mode 3 is the most dangerous one, crucial to the small-signal angular stability. (2) For mode 3 and 4, DFIG connected at node 8 is less damped than at node 16, while for mode 2, DFIG at node 16 is less damped. For mode 1, the

difference is little. Same conclusions can also be drawn from Table 2 when the DFIG was modelled as constant power sources, which demonstrates the changes of the oscillation modes are mainly due to the effect of load flow brought about by the DFIGs.

Table 4 presents the computational results of sum of participation factors of all state variables of DFIG when it was connected at node 8 and node 16 respectively. Results of DTA is given in Table 5.

Table 4 Participation Factor of the DFIG Connected at Node 8 and Node 16

	Mode 1	Mode 2	Mode 3	Mode 4
Node 8	8.6588×10^{-7}	0.0043	0.0005	0.0019
Node 16	1.2376×10^{-5}	0.0061	0.0006	0.0030

Table 5 $\Delta\bar{\lambda}_i$ by applying the DTA of the DFIG Connected at Node 8 and Node 16

	Mode 1	Mode 2	Mode 3	Mode 4
Node 8	-4.1708×10^{-6} - j1.5499×10^{-6}	-0.0140 + j0.0109	-0.0011 + j0.0013	-0.0028 + j0.0029
Node 16	-0.0001 + j0.0000	-0.0181 + j0.0124	-0.0014 + j0.0014	-0.0051 + j0.0030

From Table 4 and Table 5, it can be seen the both the participation factors and the results of $\Delta\bar{\lambda}_i, i=1,2,3,4$ computation show that (1) for DFIG at node 8 or node 16, DFIG interacts with SGs most for mode 2, and least for mode 1, (2) DFIG connected at node 16 interacts with SGs more than connected at node 8. Though the calculation of participation factor can give an estimation of dynamic interactions between the DFIG and the SGs, estimation by use of $\Delta\bar{\lambda}_i, i=1,2,3,4$ is better because $\Delta\bar{\lambda}_i, i=1,2,3,4$ can not only provide the estimation of the scale of dynamic interactions, but also indicate whether the interactions are positive to improve or negative to reduce the damping of the oscillation modes.

4. Conclusions

Grid connection of wind power can meet load increase without displacing any conventional synchronous generators in a power system. This paper investigates how this kind of grid connection of wind power affects power system small-signal angular stability. Major contribution of the paper is the proposal of applying the damping torque analysis (DTA) to estimate the impact of DFIG's dynamics on power system small-signal angular stability. The application is presented in the paper on the basis of establishment of Heffron-Phillips model of a multi-machine power system with a grid-connected DFIG. Result of applying the DTA clearly indicates that when the DFIG is modelled as a constant power injection, the effect of DFIG's dynamics is excluded. Thus the effect of load flow change brought about by

the DFIG can be identified by modelling the DFIG as a constant power source. The total impact of the DFIG is that introduced by the DFIG's dynamic interactions with SGs, which can be estimated by applying the DTA, in addition to that of load flow change brought about by the DFIG.

An example of multi-machine power system with a grid-connected DFIG is presented in the paper to demonstrate and validated the proposed application of the DTA. It is worthwhile to point out that though the application of DTA for the grid-connected DFIG is proposed in the paper on the basis of Heffron-Phillips model, it is easy to demonstrate that it is applicable for a general linearized model of a multi-machine power system where a higher-order mathematical model of synchronous generators is used.

5. References

[1] D. Gautam, V. Vittal, and T. Harbour, "Impact of Increased Penetration of DFIG-Based Wind Turbine Generators on Transient and Small Signal Stability of Power Systems," IEEE Trans. Power Syst., vol. 24, no. 3, pp. 1426-1434, Aug. 2009.

[2] J. G. Slootweg and W. L. Kling, "The impact of large scale wind power generation on power system oscillations," Elect. Power Syst. Res., vol. 67, no. 1, pp. 9-20, Oct. 2003.

[3] J. J. Sanchez-Gasca, N. W. Miller, and W. W. Price, "A modal analysis of a two-area system with significant wind power penetration," in Proc. Power Systems Conf. Expo., 2004.

[4] E. Vittal, M. O'Malley, and A. Keane, "Rotor Angle Stability With High Penetrations of Wind Generation," IEEE Trans. Power Syst., vol. 27, no. 1, pp. 353-362, Feb. 2012.

[5] E. Vittal and A. Keane, "Identification of Critical Wind Farm Locations for Improved Stability and System Planning," IEEE Trans. Power Syst., vol. 28, no. 3, pp. 2950-2958, Aug. 2013.

[6] A. Mendonca and J. A. P. Lopes, "Impact of large scale wind power integration on small signal stability," Future Power Syst., pp. 1–5, 2005.

[7] G. Tsourakis, B. M. Nomikos, and C. D. Vournas, "Contribution of Doubly Fed Wind Generators to Oscillation Damping," IEEE Trans. Energy Convers., vol. 24, no. 3, pp. 783-791, Sep. 2009.

[8] J. Quintero, V. Vittal, G. T. Heydt, and H. Zhang, "The Impact of Increased Penetration of Converter Control-Based Generators on Power System Modes of Oscillation," IEEE Trans. Power Syst., vol. 29, no. 5, pp. 2248-2256, Sep. 2014.

[9] W. G. Heffron and R. A. Phillips, "Effect of modern amplidyne voltage regulators on underexcited operation of large turbine generators," AIEE Trans. (Power Apparatus and Systems), vol. 71, no. 1, Jan. 1952.

[10] F. P. Mello and C. Concordia, "Concepts of Synchronous Machine Stability as Affected by Excitation Control," IEEE Trans. Power Appar. Syst., vol. PAS-88, no. 4, pp. 316-329, Apr. 1969.

[11] H. F. Wang, "A unified model for the analysis of FACTS devices in damping power system oscillations part III: unified power flow controller," IEEE Trans. Power Deliv., vol. 15, no. 3, pp. 978-983, Jul. 2000.

[12] H. F. Wang, F. J. Swift, and M. Li, "A unified model for the analysis of FACTS devices in damping power system oscillations part II: multi-machine power systems," IEEE Trans. Power Deliv., vol. 13, no. 4, pp. 1355-1362, Oct. 1998.

[13] H. F. Wang and F. J. Swift, "A unified model for the analysis of FACTS devices in damping power system oscillations Part I: single-machine infinite-bus power systems," IEEE Trans. Power Deliv., vol. 12, no. 2, pp. 941-946, Apr. 1997.

[14] Y N Yu, Electric Power System Dynamics. New York: Academic, 1983.

[15] A. E. Hammad, "Analysis of Power System Stability Enhancement by Static VAR Compensators," IEEE Trans. Power Syst., vol. 1, no. 4, pp. 222-227, Nov. 1986.

[16] E. Z. Zhou, "Application of static var compensators to increase power system damping", IEEE Trans. Power Syst., vol. 8, no. 2, pp. 655-661, May. 1993.

[17] H. F. Wang and F. J. Swift, "Capability of the Static Var Compensator in damping power system oscillations," in Proc. Inst. Elect. Eng. Gener. Transm. Distrib., vol. 143, Jul. 1996, pp. 353-358.

[18] W. Du, H. F. Wang, P. Ju, and R. Dunn, "Damping torque analysis for DC bus implemented damping control," European Transactions on Electrical Power, vol. 20, no. 3, pp. 277-289, Apr. 2010.

[19] M. Klein, G. J. Roger, and P. Kundur, "A fundamental study of inter-area oscillations in power systems," IEEE Trans. Power Syst., vol. 6, no. 3, pp. 914-921, Aug. 1991.

[20] G. Rogers, Power System Oscillations. Norwell, MA: Kluwer, 2000.

[21] J. B. Ekanayake, L. Holdsworth and N. Jenkins, "Comparison of 5th order and 3rd order machine models for doubly fed induction generator (DFIG) wind turbines," Elect. Power Syst. Res., vol. 67, no. 3, pp. 207-215, Dec. 2003.

[22] A. Feijóo, J. Cidrás and C. Carrillo, "A third order model for the doubly-fed induction machine," Elect. Power Syst. Res., vol. 56, no. 2, pp. 121, Nov. 2000.

[23] H. S Ko, G. G. Yoon, N. H. Kyung and W. P. Hong, "Modeling and control of DFIG-based variable-speed wind-turbine," Elect. Power Syst. Res., vol. 78, no. 11, pp. 1841-1849, Nov. 2008.

[24] L.M. Fernandez, C.A. Garcia and F. Jurado, "Comparative study on the performance of control systems for doubly fed induction generator (DFIG) wind turbines operating with power regulation," Elect. Power Syst. Res., vol. 33, no. 9, pp. 1738-1452, Sep. 2008.

[25] K. Elkington, V. Knazkins1 and M. Ghandhari, "On the stability of power systems containing doubly fed induction generator-based generation," Elect. Power Syst. Res., vol. 78, no. 9, pp. 1477-1484, Sep. 2008.

Appendix A: Heffron-Phillips model

Without loss of generality, it is assumed that a DFIG is connected at a node between node 1 and 2 in a multi-machine power system as shown by Fig. A1. From Fig. A1 it can have

$$\begin{aligned}\bar{V}_1 &= jX_{1w}\bar{I}_{1w} + \bar{V}_w = j(X_{1w} + X_w)\bar{I}_{1w} + jX_w\bar{I}_{w2} + \bar{V}_s \\ \bar{V}_2 &= jX_{w2}\bar{I}_{w2} + \bar{V}_w = jX_w\bar{I}_{1w} + j(X_{w2} + X_w)\bar{I}_{w2} + \bar{V}_s\end{aligned} \tag{A-1}$$

Matrix form of Eq.(A-1) is

$$\begin{bmatrix}\bar{I}_{1w} \\ \bar{I}_{w2}\end{bmatrix} = \begin{bmatrix} j(X_{1w} + X_w) & jX_w \\ jX_w & j(X_{w2} + X_w)\end{bmatrix}^{-1}\left(\begin{bmatrix}\bar{V}_1 \\ \bar{V}_2\end{bmatrix} - \begin{bmatrix}\bar{V}_s \\ \bar{V}_s\end{bmatrix}\right) \tag{A-2}$$

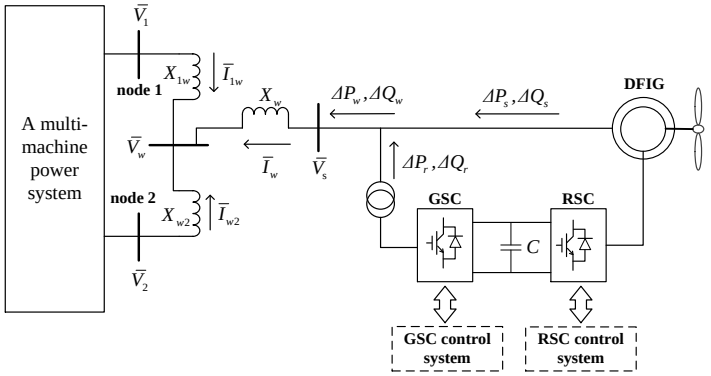

Fig. A1. *A DFIG connected to a multi-machine power system*

Assume the network equation of the N-machine power system without the DFIG connected at node s to be

$$\begin{bmatrix}0 \\ 0 \\ \bar{\mathbf{I}}_\mathbf{g}\end{bmatrix} = \begin{bmatrix}\bar{Y}_{11} & \bar{Y}_{12} & \bar{\mathbf{Y}}_{\mathbf{13}} \\ \bar{Y}_{21} & \bar{Y}_{22} & \bar{\mathbf{Y}}_{\mathbf{23}} \\ \bar{\mathbf{Y}}_{\mathbf{31}} & \bar{\mathbf{Y}}_{\mathbf{32}} & \bar{\mathbf{Y}}_{\mathbf{33}}\end{bmatrix}\begin{bmatrix}\bar{V}_1 \\ \bar{V}_2 \\ \bar{\mathbf{V}}_\mathbf{g}\end{bmatrix} \tag{A-3}$$

where $\bar{\mathbf{V}}_\mathbf{g}$ and $\bar{\mathbf{I}}_\mathbf{g}$ is the vector of terminal voltage and current of synchronous generators. With the DFIG connected, the network equation needs to be modified as follows

$$\begin{cases}\begin{bmatrix}0 \\ 0\end{bmatrix} = \begin{bmatrix}\bar{Y}_{11}' & 0 \\ 0 & \bar{Y}_{22}'\end{bmatrix}\begin{bmatrix}\bar{V}_1 \\ \bar{V}_2\end{bmatrix} + \begin{bmatrix}\bar{I}_{1w} \\ \bar{I}_{w2}\end{bmatrix} + \begin{bmatrix}\bar{\boldsymbol{Y}}_{\boldsymbol{13}} \\ \bar{\boldsymbol{Y}}_{\boldsymbol{23}}\end{bmatrix}\bar{\boldsymbol{V}}_{\boldsymbol{g}} \\ \bar{\boldsymbol{I}}_{\boldsymbol{g}} = \begin{bmatrix}\bar{\boldsymbol{Y}}_{\boldsymbol{31}} & \bar{\boldsymbol{Y}}_{\boldsymbol{32}}\end{bmatrix}\begin{bmatrix}\bar{V}_1 \\ \bar{V}_2\end{bmatrix} + \bar{\boldsymbol{Y}}_{\boldsymbol{33}}\bar{\boldsymbol{V}}_{\boldsymbol{g}}\end{cases} \tag{A-4}$$

where $\bar{Y}_{11}'$ and $\bar{Y}_{22}'$ do not include $X_{12} = X_{1w} + X_{w2}$. From Eq. (A-2) and (A-4) it can be obtained

$$\begin{aligned}\begin{bmatrix}\bar{V}_1 \\ \bar{V}_2\end{bmatrix} &= \bar{\boldsymbol{Y}}_{\boldsymbol{S}}^{-1}\left(\begin{bmatrix}\bar{V}_s \\ \bar{V}_s\end{bmatrix} - \begin{bmatrix} j(X_{1w} + X_w) & jX_w \\ jX_w & j(X_{w2} + X_w)\end{bmatrix}\begin{bmatrix}\bar{\boldsymbol{Y}}_{\boldsymbol{13}} \\ \bar{\boldsymbol{Y}}_{\boldsymbol{23}}\end{bmatrix}\bar{\boldsymbol{V}}_{\boldsymbol{g}}\right) \\ \bar{\boldsymbol{Y}}_{\boldsymbol{S}} &= \boldsymbol{I} + \begin{bmatrix} j(X_{1w} + X_w) & jX_w \\ jX_w & j(X_{w2} + X_w)\end{bmatrix}\begin{bmatrix}\bar{Y}_{11}' & 0 \\ 0 & \bar{Y}_{22}'\end{bmatrix}\end{aligned} \tag{A-5}$$

Substituting Eq.(A-5) into the second equation of (A-4) gives

$$\bar{\mathbf{Y}}_\mathbf{N}^{-1}\bar{\mathbf{I}}_\mathbf{g} = \bar{\mathbf{Y}}_\mathbf{N}^{-1}\bar{\mathbf{Y}}_\mathbf{w}\begin{bmatrix}1 \\ 1\end{bmatrix}\bar{V}_s + \bar{\mathbf{V}}_\mathbf{g} \tag{A-6}$$

where

$$\bar{\mathbf{Y}}_{\mathbf{w}} = \begin{bmatrix} \bar{\mathbf{Y}}_{31} & \bar{\mathbf{Y}}_{32} \end{bmatrix} \bar{\mathbf{Y}}_{\mathbf{s}}^{-1}$$

$$\bar{\mathbf{Y}}_{\mathbf{N}} = \bar{\mathbf{Y}}_{33} - \begin{bmatrix} \bar{\mathbf{Y}}_{31} & \bar{\mathbf{Y}}_{32} \end{bmatrix} \bar{\mathbf{Y}}_{\mathbf{s}}^{-1} \begin{bmatrix} j(X_{1w} + X_w) & jX_w \\ jX_w & j(X_{w2} + X_w) \end{bmatrix} \begin{bmatrix} \bar{\mathbf{Y}}_{13} \\ \bar{\mathbf{Y}}_{23} \end{bmatrix}$$

For the N synchronous generators, it has [14] (also refer to [14] for the definition of variables and parameters)

$$\bar{\boldsymbol{V}}_{\boldsymbol{g}} = \boldsymbol{e}^{j\delta} \boldsymbol{E}_{\boldsymbol{q}}' - \boldsymbol{j}\boldsymbol{X}_{\boldsymbol{d}}' \bar{\boldsymbol{I}}_{\boldsymbol{g}} + (\boldsymbol{X}_{\boldsymbol{q}} - \boldsymbol{X}_{\boldsymbol{d}}') \boldsymbol{e}^{j(\delta - 90^0)} \boldsymbol{I}_{\boldsymbol{q}} \tag{A-7}$$

From Eq.(A-6) and (A-7) it can have

$$\begin{aligned} &\bar{\mathbf{I}}_{\mathbf{g}} = \bar{\mathbf{Y}} [\mathbf{e}^{j\delta} \mathbf{E}_{\mathbf{q}}' + (\mathbf{X}_{\mathbf{q}} - \mathbf{X}_{\mathbf{d}}') \mathbf{e}^{j(\delta - 90^0)} \mathbf{I}_{\mathbf{q}}] + \bar{\mathbf{Y}}_{\mathbf{V}} \bar{V}_s \\ &\bar{\mathbf{Y}} = (\bar{\mathbf{Y}}_{\mathbf{N}}^{-1} + \mathbf{j}\mathbf{X}_{\mathbf{d}}')^{-1}, \bar{\mathbf{Y}}_{\mathbf{v}} = \bar{\mathbf{Y}} \mathbf{Y}_{\mathbf{N}}^{-1} \bar{\mathbf{Y}}_{\mathbf{w}} \begin{bmatrix} 1 \\ 1 \end{bmatrix} \end{aligned} \tag{A-8}$$

Thus from Eq.(A-8), terminal current of the ith generator can be written as

$$\begin{cases} I_{di} = \sum_{j=1}^{N} y_{ij} [-E_{qj}' \sin(\delta_j - \delta_i + \alpha_{ij}) + (X_{qj} - X_{dj}') I_{qj} \cos(\delta_j - \delta_i + \alpha_{ij})] + \mathrm{y}_{vi} V_s \cos(\theta - \delta_i + \alpha_i) \\ I_{qi} = \sum_{j=1}^{N} y_{ij} [E_{qj}' \cos(\delta_j - \delta_i + \alpha_{ij}) + (X_{qj} - X_{dj}') I_{qj} \sin(\delta_j - \delta_i + \alpha_{ij})] + \mathrm{y}_{vi} V_s \sin(\theta - \delta_i + \alpha_i) \end{cases} \tag{A-9}$$

where $\bar{V}_s = V_s e^{j\theta}$, $\bar{y}_{ij} = y_{ij} e^{j\alpha_{ij}}$ and $\bar{y}_{vi} = y_{vi} e^{j\alpha_i}$ is the element of $\bar{Y}$ and $\bar{\mathbf{Y}}_{\mathbf{V}}$ respectively. Linearizing Eq.(A-9) and arranging linearized equations in matrix form, it can have

$$\begin{aligned} \boldsymbol{\Delta I_d} &= \boldsymbol{F_{dd}} \boldsymbol{\Delta \delta} + \boldsymbol{G_{dd}} \boldsymbol{\Delta E_q'} + \boldsymbol{H_{dd}} \boldsymbol{\Delta I_q} + \boldsymbol{w_{dd\theta}} \Delta\theta + \boldsymbol{w_{ddV}} \Delta V_s \\ \boldsymbol{\Delta I_q} &= \boldsymbol{F_{qq}} \boldsymbol{\Delta \delta} + \boldsymbol{G_{qq}} \boldsymbol{\Delta E_q'} + \boldsymbol{H_{qq}} \boldsymbol{\Delta I_q} + \boldsymbol{w_{qq\theta}} \Delta\theta + \boldsymbol{w_{qqV}} \Delta V_s \end{aligned} \tag{A-10}$$

From Eq.(A-2) and (A-5) it can have

$$\begin{bmatrix} \bar{I}_{1w} \\ \bar{I}_{w2} \end{bmatrix} = \begin{bmatrix} j(X_{1w} - X_w) & jX_w \\ jX_w & j(X_{w2} + X_w) \end{bmatrix}^{-1} [(\bar{\boldsymbol{Y}}_{\boldsymbol{S}}^{-1} - \boldsymbol{I}) \begin{bmatrix} \bar{V}_s \\ \bar{V}_s \end{bmatrix} - \bar{\boldsymbol{Y}}_{\boldsymbol{S}}^{-1} \begin{bmatrix} j(X_{1w} - X_w) & jX_w \\ jX_w & j(X_{w2} + X_w) \end{bmatrix} \begin{bmatrix} \bar{\boldsymbol{Y}}_{\boldsymbol{13}} \\ \bar{\boldsymbol{Y}}_{\boldsymbol{23}} \end{bmatrix} \bar{\boldsymbol{V}}_{\boldsymbol{Gxy}}] \tag{A-11}$$

From Fig. 1 it can have

$$\bar{I}_w = -\bar{I}_{1w} - \bar{I}_{w2} \tag{A-12}$$

From Eq.(A-11) and (A-12) it can have

$$\bar{I}_w = \bar{\boldsymbol{Y}}_{\boldsymbol{A}} \bar{\boldsymbol{V}}_{\boldsymbol{Gxy}} + \bar{\boldsymbol{Y}}_{\boldsymbol{B}} \begin{bmatrix} \bar{V}_s \\ \bar{V}_s \end{bmatrix} \tag{A-13}$$

From Eq.(A-6) and (A-13) it can have

$$\bar{I}_w = I_{wx} + jI_{wy} == \bar{\boldsymbol{Y}}_{\boldsymbol{A}} \bar{\boldsymbol{Y}}_{\boldsymbol{N}} \bar{\boldsymbol{I}}_{\boldsymbol{Gdq}} \boldsymbol{e}^{j(\delta - 90^0)} + \left(\bar{\boldsymbol{Y}}_{\boldsymbol{B}} - \bar{\boldsymbol{Y}}_{\boldsymbol{A}} \bar{\boldsymbol{Y}}_{\boldsymbol{N}}^{-1} \bar{\boldsymbol{Y}}_{\boldsymbol{W}} \right) \begin{bmatrix} 1 \\ 1 \end{bmatrix} \bar{V}_s \tag{A-14}$$

Linearizing Eq.(A-14) gives

$$\begin{aligned} \Delta I_{wx} &= \boldsymbol{R_{x\delta}} \boldsymbol{\Delta \delta} + \boldsymbol{R_{xd}} \boldsymbol{\Delta I_d} + \boldsymbol{R_{xq}} \boldsymbol{\Delta I_q} + r_{x\theta} \Delta\theta + r_{xV} \Delta V_s \\ \Delta I_{wy} &= \boldsymbol{R_{y\delta}} \boldsymbol{\Delta \delta} + \boldsymbol{R_{yd}} \boldsymbol{\Delta I_d} + \boldsymbol{R_{yq}} \boldsymbol{\Delta I_q} + r_{y\theta} \Delta\theta + r_{yV} \Delta V_s \end{aligned} \tag{A-15}$$

The output active and reactive power of the DFIG

$$\begin{aligned} P_w &= V_{sx} I_{wx} + V_{sy} I_{wy} = I_{wx} V_s \cos\theta + I_{wy} V_s \sin\theta \\ Q_w &= V_{sy} I_{wx} - V_{sx} I_{wy} = I_{wx} V_s \sin\theta - I_{wy} V_s \cos\theta \end{aligned} \tag{A-16}$$

By linearizing Eq.(A-16) it can have

$$\begin{aligned}\Delta P_w &= R_{P\theta}\Delta\theta + R_{PV}\Delta V_s + R_{Px}\Delta I_{wx} + R_{Py}\Delta I_{wy}\\ \Delta Q_w &= R_{Q\theta}\Delta\theta + R_{QV}\Delta V_s + R_{Qx}\Delta I_{wx} + R_{Qy}\Delta I_{wy}\end{aligned} \quad \text{(A-17)}$$

From Eq.(A-15) and (A-17) it can have

$$\begin{aligned}\Delta\theta &= R_{\theta P}\Delta P_w + R_{\theta Q}\Delta Q_w + \boldsymbol{R_{\theta\delta}\Delta\delta} + \boldsymbol{R_{\theta d}\Delta I_d} + \boldsymbol{R_{\theta q}\Delta I_q}\\ \Delta V_s &= R_{VP}\Delta P_w + R_{VQ}\Delta Q_w + \boldsymbol{R_{V\delta}\Delta\delta} + \boldsymbol{R_{Vd}\Delta I_d} + \boldsymbol{R_{Vq}\Delta I_q}\end{aligned} \quad \text{(A-18)}$$

From Eq.(A-10) and (A-18) it can have

$$\begin{aligned}\boldsymbol{\Delta I_d} &= \boldsymbol{F_d\Delta\delta + G_d\Delta E_q' + w_{dP}}\Delta P_w + \boldsymbol{w_{dQ}}\Delta Q_w\\ \boldsymbol{\Delta I_q} &= \boldsymbol{F_q\Delta\delta + G_q\Delta E_q' + w_{qP}}\Delta P_w + \boldsymbol{w_{qQ}}\Delta Q_w\end{aligned} \quad \text{(A-19)}$$

Linearized model of N synchronous generators is [14] (also refer to [14] for the definition of variables and parameters)

$$\begin{cases}\boldsymbol{\Delta\dot{\delta}} = \omega_o\boldsymbol{\Delta\omega}\\ \boldsymbol{\Delta\dot{\omega}} = \mathbf{M}^{-1}(-\boldsymbol{\Delta P_g} - \mathbf{D}\boldsymbol{\Delta\omega})\\ \boldsymbol{\Delta\dot{E}_q'} = \mathbf{T_{d0}}'^{-1}(-\boldsymbol{\Delta E_q} + \boldsymbol{\Delta E_{fd}}')\\ \boldsymbol{\Delta\dot{E}_{fd}'} = -\mathbf{T_A}^{-1}\boldsymbol{\Delta E_{fd}}' - \mathbf{T_A}^{-1}\mathbf{K_A}\boldsymbol{\Delta V_g}\end{cases} \quad \text{(A-20)}$$

where

$$\begin{cases}\boldsymbol{\Delta P_g} = \mathbf{I_{q0}}\boldsymbol{\Delta E_q'} + (\mathbf{V_{d0}} - \mathbf{I_{q0}X_d'})\boldsymbol{\Delta I_d} + (\mathbf{V_{q0}} + \mathbf{I_{d0}X_q})\boldsymbol{\Delta I_q}\\ \boldsymbol{\Delta E_q} = \boldsymbol{\Delta E_q'} + (\mathbf{X_d} - \mathbf{X_d'})\boldsymbol{\Delta I_d}\\ \boldsymbol{\Delta V_g} = \mathbf{V_{g0}}^{-1}\mathbf{V_{gq0}}\boldsymbol{\Delta E_q'} - \mathbf{V_{g0}}^{-1}\mathbf{V_{gq0}X_d'}\boldsymbol{\Delta I_d} + \mathbf{V_{g0}}^{-1}\mathbf{V_{gd0}X_q}\boldsymbol{\Delta I_q}\\ \boldsymbol{\Delta V_d} = \mathbf{X_q}\boldsymbol{\Delta I_q}\\ \boldsymbol{\Delta V_q} = \boldsymbol{\Delta E_q'} - \mathbf{X_d'}\boldsymbol{\Delta I_d}\end{cases} \quad \text{(A-21)}$$

Substituting Eq.(A-19) into (A-21) it can have

$$\begin{cases}\boldsymbol{\Delta P} = \boldsymbol{K_1\Delta\delta + K_2\Delta E_q' + k_{PP}}\Delta P + \boldsymbol{k_{PQ}}\Delta Q\\ \boldsymbol{\Delta E_q} = \boldsymbol{K_3\Delta E_q' + K_4\Delta\delta + k_{EP}}\Delta P + \boldsymbol{k_{EQ}}\Delta Q\\ \boldsymbol{\Delta V_g} = \boldsymbol{K_5\Delta\delta + K_6\Delta E_q' + k_{VP}}\Delta P + \boldsymbol{k_{VQ}}\Delta Q\end{cases} \quad \text{(A-22)}$$

Thus Eq.(1) is obtained by substituting Eq.(A-22) into (A-20). Substituting Eq.(A-19) into the second equation in (A-18) gives Eq.(3).

Appendix B: Linearized model of a DFIG

Dynamic model of a DFIG can be written as [21-22, 24-25]

$$\begin{aligned}pE_{wd}' &= \omega_0\left(-\frac{R_r}{X_{rr}}E_{wd}' + sE_{wq}' + \frac{R_r X_m^2}{X_{rr}^2}I_{sq} - \frac{X_m}{X_{rr}}V_{rq}\right)\\ pE_{wq}' &= \omega_0\left(-sE_{wd}' - \frac{R_r}{X_{rr}}E_{wq}' - \frac{R_r X_m^2}{X_{rr}^2}I_{sd} + \frac{X_m}{X_{rr}}V_{rd}\right)\\ ps &= \frac{1}{J}(T_e - T_{wm})\end{aligned} \quad \text{(B-1)}$$

where $\bar{I}_s$ is the stator current, T_e and T_{wm} the electromagnetic and mechanical torque, R_r and X_{rr} the resistance and self-inductance of rotor, X_m the magnetizing inductance, J the inertia, ω_0 is the synchronous speed and

$$T_e = E_{wd}'I_{sd} + E_{wq}'I_{sq} \tag{B-2}$$

Take the direction of $\bar{V}_s$ as that of q axis of d-q coordinate of the DFIG. Thus voltage equation of stator winding of the DFIG is [22, 24]

$$V_{sd} = E_{wd}' - X'I_{sq} = 0, V_{sq} = V_s = E_{wq}' + X'I_{sd} \tag{B-3}$$

where X' is the transient inductance. Relation between stator and rotor current is [21]

$$I_{rd} = -\frac{X_{ss}}{X_m}I_{sd} - \frac{1}{X_m}V_s, I_{rq} = -\frac{X_{ss}}{X_m}I_{sq} \tag{B-4}$$

where X_{ss} is the self-inductance of stator winding. Linearization of Eq.(B-3) is

$$\Delta I_{sq} = \frac{\Delta E_{wd}'}{X'}, \Delta I_{sd} = \frac{\Delta V_s - \Delta E_{wq}'}{X'} \tag{B-5}$$

Substituting Eq.(B-5) into the linearization of Eq.(B-4) gives

$$\Delta I_{rd} = \frac{X_{ss}}{X_m X'}\Delta E_{wq}' - \frac{X' + X_{ss}}{X_m X'}\Delta V_s, \Delta I_{rq} = -\frac{X_{ss}}{X_m X'}\Delta E_{wd}' \tag{B-6}$$

Variation of DC voltage of the AC/DC converter and its effect on power system small-signal stability is very small. For the simplicity of derivation, it is assumed to be a constant (If considered, similar derivation can be carried out and conclusions of the paper will not be affected). Hence the dynamics of converter and network-side converter control system are not included in the discussions. Configuration of rotor-side converter control system is shown by Fig. B1 [23-24], where superscript ref indicates the reference of associated signal, P_s and Q_s is the stator active and reactive power output of the DFIG respectively.

$$P_s = V_{sd}I_{sd} + V_{sq}I_{sq} = V_s I_{sq}, Q_s = V_{sq}I_{sd} - V_{sd}I_{sq} = V_s I_{sd} \tag{B-7}$$

By using Eq.(B-5), linearization of Eq.(B-7) is obtained to be

$$\begin{aligned} \Delta P_s &= V_{s0}\Delta I_{sq} + I_{sq0}\Delta V_s = \frac{V_{s0}}{X'}\Delta E_{wd} + I_{sq0}\Delta V_s \\ \Delta Q_s &= V_{s0}\Delta I_{sd} + I_{sd0}\Delta V_s = -\frac{V_{s0}}{X'}\Delta E_{wq} + (\frac{V_{s0}}{X'} + I_{sd0})\Delta V_s \end{aligned} \tag{B-8}$$

where subscript 0 denotes steady-state value of the associated variable.

Denote the transfer function of active and reactive power PI controller by $K_{pd}(p)$ and $K_{pq}(p)$, that of direct and quadrature current by $K_{id}(p)$ and $K_{iq}(p)$ respectively. From Fig. B1 and Eq.(B-8) it can have

$$\Delta I_{sq}^{ref} = -K_{pq}(p)\Delta P_s = -K_{pq}(p)\frac{V_{s0}}{X'}\Delta E_{wd}' - K_{pq}(p)I_{sq0}\Delta V_s$$
$$\Delta I_{sd}^{ref} = -K_{pd}(p)\Delta Q_s = K_{pd}(p)\frac{V_{s0}}{X'}\Delta E_{wq}' - K_{pd}(p)(\frac{V_{s0}}{X'} + I_{sd0})\Delta V_s \quad \text{(B-9)}$$

From Fig. B1 and Eq.(B-9) it can have

$$\Delta I_{rd}^{ref} = -\frac{X_{ss}}{X_m}\Delta I_{sd}^{ref} - \frac{\Delta V_s}{X_m} = -K_{pd}(p)\frac{X_{ss}V_{s0}}{X_m X'}\Delta E_{wd}' + \frac{K_{pq}(s)X_{ss}(V_{s0} + X'I_{sd0}) - X'}{X_m X'}\Delta V_s$$
$$\Delta I_{rq}^{ref} = -\frac{X_{ss}}{X_m}\Delta I_{sq}^{ref} = K_{pq}(s)\frac{X_{ss}V_{s0}}{X_m X'}\Delta E_{wd}' + K_{pd}(s)\frac{X_{ss}I_{sq0}}{X_m}\Delta V_s \quad \text{(B-10)}$$

Hence from Fig. B1 and Eq.(B-10) it can have

$$\Delta V_{rd} = K_{id}(p)\Delta I_{rd}^{*} - K_{id}(p)\Delta I_{rd} + s_0(\frac{X_m^2}{X_{ss}} - X_{rr})\Delta I_{rq} + (\frac{X_m^2}{X_{ss}} - X_{rr})I_{rq0}\Delta s$$
$$= s_0\frac{X_{ss}X_{rr} - X_m^2}{X_m X'}\Delta E_{wd}' - \left[K_{id}(s)K_{pd}(s)\frac{X_{ss}V_{s0}}{X_m X'} + K_{id}(s)\frac{X_{ss}}{X_m X'}\right]\Delta E_{wq}' + (\frac{X_m^2}{X_{ss}} - X_{rr})I_{rq0}\Delta s + \left[\begin{array}{l} K_{id}(s)\dfrac{K_{pq}(s)X_{ss}(V_{s0} + X'I_{sd0}) - X'}{X_m X'} \\ +K_{id}(s)\dfrac{X' + X_{ss}}{X_m X'}\end{array}\right]\Delta V_s$$
$$\Delta V_{rq} = K_{iq}(p)\Delta I_{rq}^{*} + s_0(X_{rr} - \frac{X_m^2}{X_{ss}})\Delta I_{rd} - K_{iq}(p)\Delta I_{rq} + \left[(X_{rr} - \frac{X_m^2}{X_{ss}})I_{rd0} + \frac{X_m}{X_{ss}}V_{s0}\right]\Delta s + s_0\frac{X_m}{X_{ss}}\Delta V_s$$
$$= \left(K_{iq}(s)K_{pq}(s)\frac{X_{ss}V_{s0}}{X_m X'} + K_{iq}(s)\frac{X_{ss}}{X_m X'}\right)\Delta E_{wd}' + s_0\frac{X_{rr}X_{ss} - X_m^2}{X_m X'}\Delta E_{wq}' + \left[(X_{rr} - \frac{X_m^2}{X_{ss}})I_{rd0} + \frac{X_m}{X_{ss}}V_{s0}\right]\Delta s$$
$$+\left[K_{iq}(s)K_{pd}(s)\frac{X_{ss}I_{sq0}}{X_m} - s_0(X_{rr} - \frac{X_m^2}{X_{ss}})\frac{X' + X_{ss}}{X_m X'} + s_0\frac{X_m}{X_{ss}}\right]\Delta V_s \quad \text{(B-11)}$$

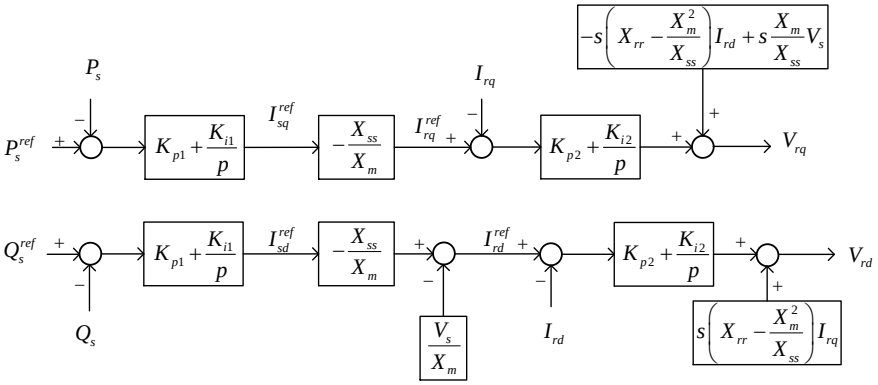

Fig. B1. *Configuration of rotor-side converter control system*

Eq.(5) is the compact form of Eq.(B-11). By using Eq.(B-5), linearization of Eq.(B-2) is obtained to be

$$\Delta T_e = (I_{sd0} + \frac{E_{wq0}'}{X'})\Delta E_{wd}' + (I_{sq0} - \frac{E_{wd0}'}{X'})\Delta E_{wq}' + \frac{E_{wd0}'}{X'}\Delta V_s \quad \text{(B-12)}$$

By using Eq.(B-11) and (B-12) and linearizing (B-1), Eq.(4) is obtained.

The rotor active and reactive power output of the DFIG generator are

$$P_r = V_{rd}I_{rd} + V_{rq}I_{rq}, Q_r = 0 \quad \text{(B-13)}$$

Linearizing Eq.(B-13) it can have

$$\Delta P_r = I_{rd0}\Delta V_{rd} + I_{rq0}\Delta V_{rq} + V_{rd0}\Delta I_{rd} + V_{rq0}\Delta I_{rq}, \Delta Q_r = 0 \quad \text{(B-14)}$$

Linearized total output active and reactive power of DFIG generator is

$$\Delta P_w = \Delta P_s + \Delta P_r, \Delta Q_w = \Delta Q_s \tag{B-15}$$

By substituting Eq. (B-6), (B-8), (B-11), (B-14) and (B-15), Eq.(7) is obtained.

Appendix C: Proof of Eq.(12)

From Eq.(2), (3) and (8), the state equation of the closed-loop system can be obtained as

$$\begin{bmatrix} p\boldsymbol{X}_g \\ p\boldsymbol{X}_w \\ p\boldsymbol{X}_c \end{bmatrix} = \boldsymbol{A}\begin{bmatrix} \boldsymbol{X}_g \\ \boldsymbol{X}_w \\ \boldsymbol{X}_c \end{bmatrix}, \ \boldsymbol{A} \in R^{M\times M} \tag{C-1}$$

where $\boldsymbol{X}_c$ is the vector of state variables of control system of the DFIG generator. If $\bar{\lambda}_j = -\xi_j + j\omega_j$ and $\bar{\boldsymbol{v}}_j$, $j = 1, 2, \cdots M$ is the eigenvalue and associated right eigenvector of state matrix $\boldsymbol{A}$, it should have

$$\boldsymbol{X}_g = \sum_{j=1}^{M} \frac{\bar{\boldsymbol{v}}_{\boldsymbol{jg}} \bar{a}_j}{p - \bar{\lambda}_j}, \ \Delta\omega_k = \sum_{j=1}^{M} \frac{\bar{v}_{jk} \bar{a}_j}{s - \bar{\lambda}_j} \tag{C-2}$$

where $\bar{\boldsymbol{v}}_{\boldsymbol{jg}}$ is the vector consisted of elements of $\bar{\boldsymbol{v}}_j$ corresponding to $\boldsymbol{X}_g$, $\bar{v}_{jk}$ is the element of $\bar{\boldsymbol{v}}_j$ corresponding to $\Delta\omega_k$. From Eq.(3) and (8), it can have

$$\Delta V_s = \frac{\boldsymbol{C}_g \boldsymbol{\Delta X}_g}{1 - d_{g1} G_{wP}(p) - d_{g2} G_{wQ}(p)} \tag{C-3}$$

Thus

$$\frac{\Delta V_s}{\Delta\omega_k} = \frac{\dfrac{1}{1 - d_{g1} G_{wP}(p) - d_{g2} G_{wQ}(p)} \mathbf{C}_\mathbf{g} \sum_{j=1}^{M} \dfrac{\bar{\mathbf{v}}_{\mathbf{jg}} \bar{a}_j}{p - \bar{\lambda}_j}}{\sum_{j=1}^{M} \dfrac{\bar{v}_{jk} \bar{a}_j}{s - \bar{\lambda}_j}} = \frac{\dfrac{1}{1 - d_{g1} G_{wP}(p) - d_{g2} G_{wQ}(p)} (p - \lambda_i) \mathbf{C}_\mathbf{g} \sum_{j=1}^{M} \dfrac{\bar{\mathbf{v}}_{\mathbf{jg}} \bar{a}_j}{p - \bar{\lambda}_j}}{(p - \lambda_i) \sum_{j=1}^{M} \dfrac{\bar{v}_{jk} \bar{a}_j}{s - \bar{\lambda}_j}} \tag{C-4}$$

Let $p = \bar{\lambda}_i$ in the above equation, Eq.(12) is obtained.

Appendix D: DFIGs' parameters

Examples in the paper are for the purpose of demonstration and validation of the proposed method. Hence the parameters of DFIGs used are same to be

$$T_J = 8s, D = 0, R_s = 0, R_r = 0.0145, X_m = 2.4012, X_s = 0.1784, X_r = 0.1225, K_{p1} = 0.2, K_{i2} = 12.56, K_{p2} = 1, K_{i2} = 62.5$$